2008 IEEE International Conference on
Robotics and Automation
Pasadena, CA, USA, May 19-23, 2008

Nonlinear modeling of low cost force sensors

C. Lebossé, B. Bayle, M. de Mathelin
LSIIT, UMR ULP-CNRS 7005
Pole API, Bd. S. Brant, 67412 Illkirch, France

P. Renaud
LGeCo, INSA-Strasbourg
67084 Strasbourg, France

***Abstract*— In this paper, nonlinear modeling of low cost force sensors is considered for force control applications in robotic or biomechanical applications. Commercial force sensors are often expensive, with a limited use in severe conditions such as the presence of a strong magnetic field. On the contrary, thin film piezoresistive sensors such as the Tekscan Flexiforce and the Interlink FSR sensors are of low cost and can be considered in such an environment. Only a few information is however available on their dynamic properties. We therefore provide an experimental study of their dynamic behavior, showing nonlinear properties. Identification is then achieved, and a compensation model is proposed. A force control experiment is finally presented to evaluate the compensation scheme.**

I. Introduction

In many robotic and biomechanical applications, force measurement is needed to ensure safety and comfort in human/robot interaction, for instance in medical robotics [1] [2], and to analyse force distribution in common human movements as grasping [3] or walking [4].

Different types of force sensors have been used up to now in such contexts, differing by their technology:

- strain gauge sensors consist of a pattern of strain gauges mounted on a deformable structure. The force applied on the sensor induces strains in the structure which are evaluated by strain gauges. Foil or silicon strain gauges can be used, like in the ATI sensors, used in several medical robotic applications [5] [2].
- piezoelectric force sensors, such as the LIVM force sensor (Dytran Instruments Inc. CA, US), contain thin piezoelectric crystals generating analog voltage signals in response to applied dynamic forces.
- optical force sensors are based on the evaluation of the deformation of a structure either with light intensity measurement over optical fibers [6] [7] or Fiber Bragg Grating [8]. Such sensors present the advantage of being insensitive to the presence of a magnetic field.
- thin film piezoresistive force sensors such as the FSR (Interlink Electronics, Camarillo, CA, US) and the Flexiforce (Tekscan Inc., Boston, MA, US) sensors have their resistance varying with the applied force. They exhibit a lower accuracy than the other types, but their very small thickness allows a placement directly in contact with a human, for example for tactile sensing [3] [9].

Thin film piezoresistive sensors have interesting properties, and their low cost enables to consider the integration of a large number of sensors for instance in a collision detection task. Furthermore, the Flexiforce sensors have been demonstrated to be insensitive to magnetic fields [10]. For a growing number of medical applications involving the placement of the patient inside an MRI system [11] [12] or under pulsed magnetic fields [1], these sensors may therefore be of great interest in the case of force control tasks which do not require a strong accuracy.

For a control task, the dynamic behavior of the used sensor has to be evaluated. To our knowledge, only a few work has been performed for these sensors. Vecchi et al. [13] achieved a comparison of the respective performances of both commercial piezoresistive force sensors FSR and Flexiforce, but only in static conditions.

In this paper, we present an experimental analysis of the dynamic behavior of such sensors. The presence of nonlinearities is outlined, and a model is then identified to allow a compensation. This study aims therefore at enhancing the application field of these sensors to force control tasks.

The paper is organized as follows. In section II, the experimental set-up and protocol are first presented. The sensor calibration as well as the analysis of their static response are then carried out in section III. In section IV, the nonlinearities of the dynamic behavior are outlined before a complete characterization and identification. In section V, a force control experimentation is performed, in order to prove that it is possible to use the proposed model to compensate for the nonlinearities. Conclusion and perspective on this work are then finally given.

II. Experimental set-up

In the following, both Interlink FSR and Tekscan Flexiforce sensors are evaluated.

The FSR is a thin-film device consisting of two conducting interdigitated patterns deposited on a thermoplastic sheet, facing another sheet which contains a conductive polyetherimide film. A spacer placed between the plastic sheets permits the two sheets to make electrical contact when the force is applied. Otherwise, in the unloaded state, it causes the sensor to have infinite impedance. As the applied force increases, the two layers compress each other, thus, increasing the contact area and decreasing the electrical resistance.

The Flexiforce sensor is made of two layers of substrate, such as a polyester film. On each layer, a conductive material

978-1-4244-1647-9/08/$25.00 ©2008 IEEE.

is applied, followed by a layer of pressure-sensitive ink. The active sensing area is defined by a silver circle on the top of the pressure-sensitive ink. When the sensor is unloaded, its electrical resistance is very high. When a force is applied to the sensor, this resistance decreases.

As mentioned in the introduction, control of the contact force between a human and a robot is among the potential applications of the integration of such sensors. We consider the case of a robotic system designed to position on the head of a patient a stimulation coil emitting a strong magnetic field [1]. In that case, for comfort reasons, force has to be controlled to remain below 5N. To be compatible with the application, two sensors were selected: an A-201 Flexiforce sensor, with an optimal force range of 4.5N, and a FSR sensor, with a unique range of 100N. The geometry of their sensing areas is compatible with the application. The Flexiforce has a 10mm diameter circular active area and the FSR has a 38mm square active area (Fig. 1). Since

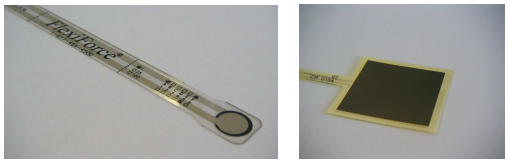

Fig. 1. On the left the Flexiforce A-201 sensor, on the right the FSR sensor

force evaluation is obtained for both sensors by a resistance variation, the sensitivity can be adjusted by modifying the electric circuit connected to the sensors. This circuit is based on an inverting operational amplifier arrangement, to produce an analog output based on the sensor resistance and a fixed resistance. This latter one is chosen for each sensor to obtain a voltage between 0 and 10 V for a force range around 7N. An ATI Industrial Automation Nano17 force sensor (Model SI12/0.12) is used as a reference during the calibration and the dynamic measurements. The sensing range of this sensor is 17N with a resolution of 0.025N.

The dynamic testing of the sensors includes a force excitation with a sine shape in order to evaluate bandwidth. To do so, a custom bench test has been manufactured (Fig. 2). It is composed of a Maxon DC motor on which an eccentric wheel is mounted, which induces the movement of a trolley on a linear guide (cam and follower system). This movement is converted into a force applied on both sensors by means of a spring. The material of the elements close to the sensor is chosen to be insensitive to magnetic fields. It could then be verified that both sensors are non-sensitive to a magnetic field, using the magnetic coil described in [1].

III. Calibration and Static Response

In this section, the calibration phase and the evaluation of the static properties, *i.e.* hysteresis, repeatability and time drift are presented.

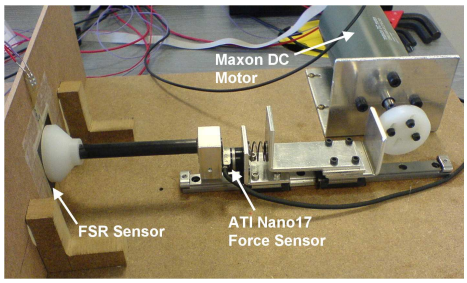

Fig. 2. The dedicated test bench

A. Calibration

Each force sensor has been calibrated individually on a rigid plane using the Nano17 force sensor. An increasing then decreasing force was manually and continuously applied two times over the 7N force range. The sensors and the Nano17 outputs were sampled at a frequency of 50Hz for a period of 120s.

Fig. 3, left, shows a calibration curve obtained with the Flexiforce sensor. One can notice that the response does

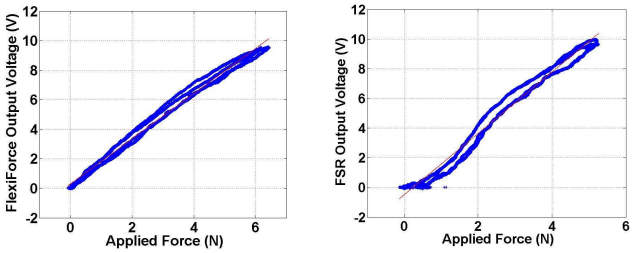

Fig. 3. Calibration of the Flexiforce (left) and the FSR (right) sensors.

not decline over 4.5N, the sensor given range. The sensor response exhibits a hysteresis below 10% with regards to the full scale of 7N. The mean calibration error is about 5%, with a standard deviation of 2.8%. A linear model is identified from the calibration curve:

$$F = GU + F_0 \quad (1)$$

with F the applied force, U the measured output voltage. The gain G=0.65N/V and the offset F_0=-0.19N.

Fig. 3 right shows a calibration curve obtained with the FSR sensor. One can notice that the linearity of the response is not as good as the one obtained with the Flexiforce. The sensor response exhibits a hysteresis below 8% with regards to the full scale of 7N. The mean calibration error is about 7%, with a standard deviation of 3%. The linear model of equation (1) is identified with G=0.48N/V and F_0=0.24N.

B. Repeatability

The repeatability of the two sensors has also been evaluated. Ten different loads were applied ten times on each

sensor. The results are presented in Fig. 4. The mean error is 3.6% for the Flexiforce sensor and 2.1% for the FSR sensor.

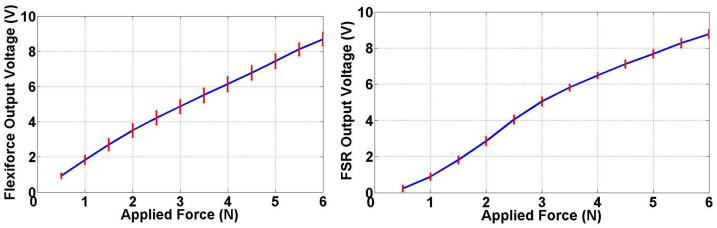

Fig. 4. Repeatability of the Flexiforce (left) and FSR (right) sensors.

C. Time drift

The performance of the two sensors in terms of time drift of the their outputs has also been evaluated. A constant load of 3N was applied on the sensors for 20 minutes. The results are presented in Fig. 5. The time drift is inferior to 6% for the Flexiforce sensor and inferior to 4% for the FSR sensor.

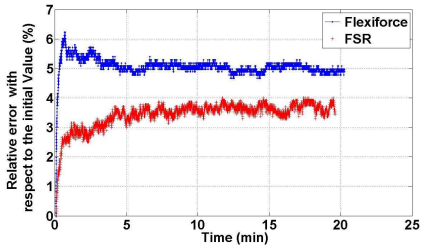

Fig. 5. Time drift for the two sensors. A constant load of 3N is applied for 20 minutes.

D. Static properties

The results of this static evaluation show that for this force range both sensors responses are quite equivalent. However, the Flexiforce sensor response presents a better linearity, while the performance of the FSR in terms of repeatability and time drift seems slightly better for the evaluated force range. These results are slightly different from those obtained by Vecchi *et al.* in [13]. In that paper, the Flexiforce sensor demonstrated a better overall performance. This could be due to the force range considered here which is only 7N compared to the 30N evaluated through their analysis.

IV. Nonlinearities Characterization and Identification

A. Dynamic response

Considering their step response, both sensors could be identified as first-order systems, with a time constant of 30ms for the Flexiforce sensor and 35ms for the FSR, which corresponds to a cut-off frequency around 30Hz. However, the examination of the response to a sinusoidal excitation, with a frequency far below the estimated cut-off frequency, gives rise to the presence of a significant nonlinearity. Indeed, a decline with time of the sensor response immediately appears whatever the sinusoïdal excitation is. Fig. 6 shows a typical response of the two sensors. The signal decrease with time only affects the maxima of the sensor response, whereas the minima remain at the same level. For the Flexiforce sensor, the decrease is rather exponential with a loss that can reach 80% of the sensor initial response after 20 min, depending on the force range and the frequency. For the FSR sensor, the decrease is rather linear with a loss that can reach 30%. This phenomenon appears even with low frequencies and force ranges: with the Flexiforce for instance, a loss of 79% can be observed with an excitation of 1.5N in amplitude and 0.05Hz in frequency. Likewise, a loss of 68% is obtained with a frequency of 0.5Hz and an amplitude of 0.44N.

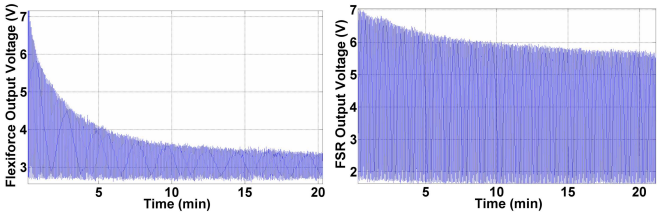

Fig. 6. Sensor response for a sinusoïdal excitation applied during 20 minutes at a frequency of 0.25Hz with a force range between 1.3 and 4.4N.

In order to be able to use these sensors in force control applications, it is required to compensate for these nonlinearities. An experimental characterization has therefore been achieved to identify a model of these nonlinearities.

B. Nonlinearities identification

In a first step, it is needed to evaluate the sensor signal decrease as a function of the sinusoidal excitation. This excitation $F(t)$ can be defined by its frequency f, its mean value m and its amplitude A:

$$F(t) = Asin(2\pi ft) + m, \text{with} \quad m \geq A \tag{2}$$

For each sensor, three series of measurements have been performed, each one corresponding to the variation of one of the three parameters (f, m, A). The range for the mean value and the amplitude of the applied force has been selected in order to be able to handle any excitation between 0 and 4.5N, *i.e.* the Flexiforce force range. A range between 0 and 4Hz has been chosen for the frequency, considering the fact that the signal loss is already very important for such frequencies and thus it is not relevant to go beyond this range.

For each sensor response, the value of the minima U_{min} of U, which remains constant is removed from the output response. The maxima of the response are then extracted and used as raw data for a curve fitting.

1) Flexiforce model identification: An exponential decrease is chosen to describe the signal maxima loss, leading to the following expression for the maxima of the output voltage response:

$$U_{max}(t) = U_{min} + ae^{-bt} + c \quad (3)$$

The expression of U_{min} can easily be inferred from the force sensor characterization and the input features:

$$U_{min} = \frac{m - A - F_0}{G} \quad (4)$$

The Tables I, II and III present the variations of the parameters a, b, and c with f, A, and m, as well as the root mean square error RMSE for each fit. From the analysis of these variations,three models are inferred: b is considered only dependent of the frequency f, a is considered as a function of the amplitude A and the ratio $\frac{c}{a}$, which reflects the signal loss intensity, mainly depends on A. After identification, three equations are obtained:

f (Hz)	0.05	0.15	0.25	0.5	1
a	3.244	3.368	3.479	3.596	2.869
$b(.10^3)$	7.460	5.575	7.013	7.072	8.099
c	0.676	0.693	0.889	0.825	0.633
RMSE	0.072	0.102	0.056	0.064	0.083
f (Hz)	1.5	2	2.5	3	4
a	1.999	3.128	4.064	2.377	2.16
$b(.10^3)$	5.57	1.22	1.89	8.57	4.32
c	0.825	0.532	0.447	0.591	0.832
RMSE	0.061	0.079	0.039	0.091	0.062

TABLE I
VARIATIONS OF a, b AND c WITH f FOR THE FLEXIFORCE SENSOR

A (N)	0.441	0.784	0.981	1.226	1.471	1.766
a	0.4421	1.090	1.979	2.188	3.390	4.189
$b(.10^3)$	9.039	3.974	8.473	7.564	5.128	4.855
c	0.297	0.904	0.672	0.735	0.485	0.466
RMSE	0.006	0.113	0.043	0.053	0.076	0.053

TABLE II
VARIATIONS OF a, b AND c WITH A FOR THE FLEXIFORCE SENSOR.

m (N)	1.766	1.962	2.452	2.943	3.433
a	1.857	1.726	1.287	1.068	1.136
$b(.10^3)$	6.759	6.178	6.795	8.352	7.275
c	0.563	0.533	0.566	0.385	0.518
RMSE	0.0486	0.0375	0.0390	0.0256	0.0332

TABLE III
VARIATIONS OF a, b AND c WITH m FOR THE FLEXIFORCE SENSOR.

$$a = 0.8839A^2 + 0.8655A \quad (5)$$

$$b = 0.0019f + 0.0056 \quad (6)$$

$$\frac{c}{a} = \frac{1}{1 + 1.377A^2} \quad (7)$$

These equations allow us to get the best results in terms of identification, while satisfying the physical meaning of the parameters: $a \geq 0$, $b \geq 0$, $\frac{c}{a} \geq 0$ and $a = 0$ when $A = 0$, *i.e.* when no force variation is applied. The proposed model enables us to estimate the overall sensor output observed during the experiments with a mean error of 13%. The three parameters a, b and c estimated with the experiments can be computed with respectively 17%, 30% and 14%.

The model of the Flexiforce sensor output voltage is finally given by the following expression:

$$U_{model}(t) = \frac{1}{2}(ae^{-bt} + c)(sin(2\pi ft) + 1) + U_{min} \quad (8)$$

2) FSR model identification: For each experimentation, the linear model was the only one to provide a fit for the maxima decrease, even for a one hour experimentation, which is the upper limit for our application. It is therefore used for the description of the maxima of the output voltage response:

$$U_{max}(t) = at + b + U_{min} \quad (9)$$

The Tables IV, V and VI present the variations of the parameters a and b with the frequency f, the amplitude A, and the mean value m, as well as the root mean square error RMSE for each fit. From the analysis of these variations, two models are inferred: a is considered as a function of the amplitude A and b is considered as a function of the

f (Hz)	0.05	0.15	0.25	0.5	1
$a(.10^4)$	-4.0	-6.5	-10.6	1.07	-4.1
b	5.298	7.130	5.0	6.351	4.8130
RMSE	0.033	0.061	0.448	0.087	0.035
f (Hz)	1.5	2	2.5	3	4
$a(.10^4)$	-10.5	-4.21	-7.29	-11.5	-3.8
b	5.890	5.167	5.345	3.967	6.0440
RMSE	0.130	0.045	0.025	0.171	0.139

TABLE IV
VARIATIONS OF a AND b WITH f FOR THE FSR SENSOR.

A (N)	0.441	0.784	0.981	1.226	1.471	1.766
$a(.10^4)$	-1.66	-0.721	-1.72	-3.72	-1.68	-5.85
b	1.989	3.786	3.980	5.450	5.50	6.386
RMSE	0.0765	0.0396	0.0263	0.0691	0.0381	0.0852

TABLE V
VARIATIONS OF a AND b WITH A FOR THE FSR SENSOR.

m (N)	1.766	1.962	2.452	2.943	3.433
$a(.10^4)$	-1.66	2.57	-6.66	-1.98	-0.739
b	5.589	3.617	3.555	1.728	1.747
RMSE	0.0766	0.0341	0.0627	0.0511	0.0361

TABLE VI
VARIATIONS OF a AND b WITH m FOR THE FSR SENSOR.

amplitude A and mean value m, after identification. Two equations are obtained:

$$a = -1.187e^{-4}A^2 + -7.074e^{-5}A \quad (10)$$

$$b = 3.221A - 2.110m + 6.05 \quad (11)$$

These equations allow us to get the best results in terms of identification while satisfying the physical meaning of the parameters: $a \geq 0$, $b \geq 0$ and $a = 0$ when $A = 0$, *i.e.* when no force variation is applied. The proposed model enables us to estimate the overall sensor output observed during the experiments with a mean error of 14%. The parameter b estimated with the experiments can be computed with an average error in the order of 12%, while the parameter a can be computed with an average error of 48%. This result means that the linear decline may slightly depend on other physical phenomena responsible for the observed nonlinearities.

The model of the FSR sensor output voltage is finally given by the following expression:

$$U_{model}(t) = \frac{a+b}{2}(sin(2\pi ft) + 1) + U_{min} \quad (12)$$

The compensation model of each sensor enables to construct an estimation $F_{est}(t)$ of the real force applied from the altered force measured $F_{meas}(t)$, for any sinusoidal excitation. For instance, when using the Flexiforce sensor, the estimated force is given by the following expression:

$$F_{est}(t) = \frac{2A}{G(ae^{-bt} + c)}(F_{meas}(t) - m + A) + m - A \quad (13)$$

It must be noticed that the three parameters (f, m, A) of the excitation, which are required to compute $F_{est}(t)$, could be estimated in-line by analyzing the beginning of $F_{meas}(t)$.

V. Force control with sensor nonlinearities compensation

In order to show that it is possible to use the proposed models to compensate for the nonlinearities of such sensors, a force control experimentation is presented. We focus on the Flexiforce sensor, which nonlinearities are the strongest. The test bench introduced in section II has been used with the force control scheme of [14] showed in Fig. 7, where $F^*(t)$ is the desired force, F the measured force, K_I the gain of the force controller, x is the position, q the angular value and IKM the inverse kinematic model of the system. The compensation block use the identified model to construct an estimation of the real force applied.

The eccentric wheel was set to get a possible force range between 0.8N and 4.1N with half a rotation. A sinusoïdal desired force with a frequency of 0.5Hz and a force range between 1.1N et 3.2N was chosen in order to get the nonlinearities of the Flexiforce sensor previously characterized. The force regulation is characterized by a bounded force tracking error which can be made small by adjusting K_I. This means that the desired force is the force applied on the sensor when

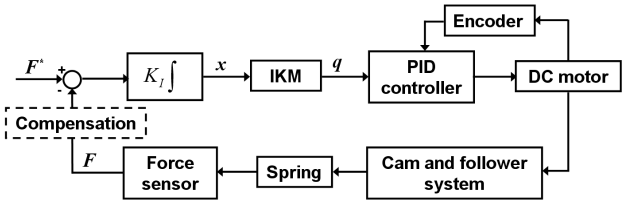

Fig. 7. Force control scheme.

the sensor response exhibits no non-linearity. It is the case when the Nano17 sensor is used for the force control, for example, as it has a much higher bandwidth. The Nano17 is used here as a reference to see the force really applied on both sensors.

Fig. 8 shows the responses of both Nano17 and Flexiforce sensors during the force control experimentation. The response of the Nano17 sensor is characterized by a rise of both maxima and minima until they reach a value corresponding to the maximum force that can be applied by the system, when the eccentric wheel has performed half a rotation. The Flexiforce response shows an exponential decline of the maxima, but smaller than the one observed previously, and a symmetric rise of the minima. These responses are due to sensor defaults and to the compensation of the nonlinearities that the force controller tries to perform. Indeed, when the maxima of the Flexiforce response decrease, the controller induces a greater rotation of the wheel in order to apply a stronger force, leading to the rise of the maxima in the Nano17 response. However, the controller is not able to compensate for all the decline and thus a positive error is cumulated, leading to a rise of the minima as well. Finally, both rises reach a saturation when the extreme position of the wheel is attained which leads to a constant signal when the wheel remains in the same position, in less than 150s.

Fig. 9 shows the responses obtained when the proposed model is used to compensate for the nonlinearities. Thanks to the compensation the Nano17 response almost corresponds to the desired force after a certain settling time for the maxima while the minima remain always constant. The mean error on maxima and minima is presented in Table VII. Moreover, the performance of the compensation is maintained during the 300s of the experiments, whereas a constant signal was obtained in less than 150s without.

	Without compensation		With compensation	
	Min	Max	Min	Max
Mean Error	134.1%	26.9%	4.5%	7.5%
Std Deviation	96.1%	6.3%	0.5%	5.5%

TABLE VII
CONTROL ERROR ON MAXIMA AND MINIMA OF THE RESPONSE

This experimentation shows that the proposed model en-

ables to compensate most of the sensors nonlinearities, making it possible to use them in force control applications.

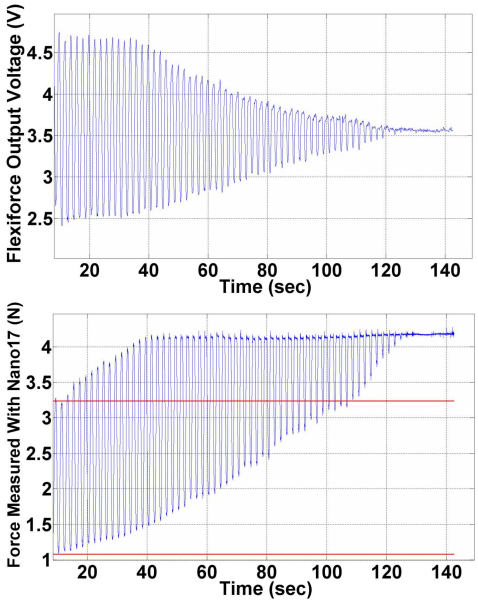

Fig. 8. Force measured with Nano17 and Flexiforce sensors during a force control experimentation without any compensation.

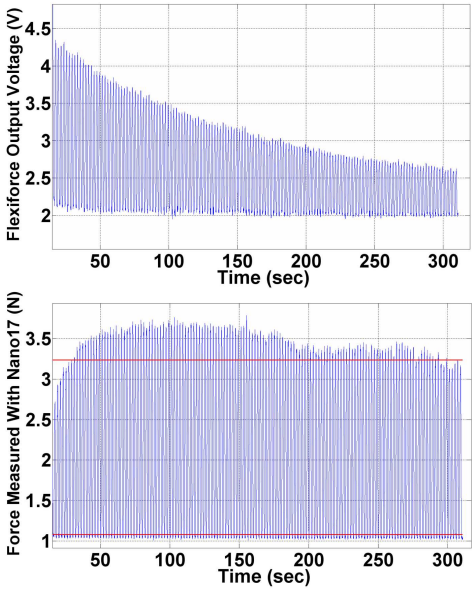

Fig. 9. Force measured with Nano17 and Flexiforce sensors during a force control experimentation with nonlinearities compensation.

VI. Conclusion

In this paper, the nonlinear modeling of two commercial force sensors is considered for force control applications. Theses sensors are of low cost and can be used in the presence of a strong magnetic field, which is of great interest for medical applications. An experimental study of their static and dynamic behavior is provided. In particular, strong nonlinearities in their dynamic behavior are shown. These nonlinearities are identified and a compensation model is proposed. A force control experiment finally gives a first proof of the compensation scheme efficiency. Further investigations will now be achieved to evaluate the sensor behavior for dynamic excitations with a broader frequency spectrum, that can occur in force regulation tasks.

References

[1] C. Lebossé, P. Renaud, B. Bayle, M. de Mathelin, O. Piccin, E. Laroche, and J. Foucher, "Robotic image-guided transcranial magnetic stimulation," in *Computer Assisted Radiology and Surgery (CARS)*, (Osaka, Japan), June 2006.

[2] G. Duchemin, E. Dombre, F. Pierrot, P. Poignet, and E. Dégoulange, "Scalpp: a safe methodology to robotize skin harvesting," in *MICCAI*, (Utrecht, The Netherlands), pp. 309–316, October 2001.

[3] Y. Kong and B. Lowe, "Optimal cylindrical handle diameter for grip force tasks," *International Journal of Industrial Ergonomics*, vol. 35, no. 6, pp. 495–507, 2005.

[4] A. Faivre, *Conception et validation d'un nouvel outil d'analyse de la marche*. PhD thesis, Université de Franche Comté, 2003.

[5] R. H. Taylor, P. S. Jensen, L. L. Whitcomb, A. C. Barnes, R. Kumar, D. Stoianovici, P. K. Gupta, Z. Wang, E. de Juan, and L. R. Kavoussi, "A steady-hand robotic system for microsurgical augmentation," in *MICCAI*, pp. 1031–1041, 1999.

[6] D. Chapuis, R. Gassert, L. Sache, E. Burdet, and H. Bleuler, "Design of a simple mri/fmri compatible force/torque sensor," in *IEEE International Conference on Intelligent Robots and Systems*, vol. 3, (Sendai, Japan), pp. 2593–2599, September 2004.

[7] N. Takahashi, M. Tada, J. Ueda, Y. Matsumoto, and T. Ogasawara, "An optical 6-axis force sensor for brain function analysis using fmri," in *IEEE International Conference on Sensors*, (Toronto, Canada), pp. 253–258, October 2003.

[8] Y.-L. Park, K. Chau, R. Black, and M. Cutkosky, "Force sensing robot fingers using embedded fiber bragg grating sensors and shape deposition manufacturing," in *IEEE International Conference on Robotics and Automation*, (Roma, Italy), pp. 1510–1516, April 2007.

[9] M. C. F. Castro and A. Cliquet, "A low-cost instrumented glove for monitoring forces during object manipulation," *IEEE Transactions on Rehabilitation Engineering*, vol. 5, pp. 140–147, June 1997.

[10] A. Balakrishnan, D.F., Kacher, A. Slocum, C. Kemper, and S. K. Warfield, "Smart retractor for use in image guided neurosurgery," in *Summer Bioengineering Conference*, (Key Biscayne, Florida), June 2003.

[11] A. Patriciu, D. Petrisor, M. Muntener, D. Mazilu, M. Schär, and D. Stoianovici, "Automatic brachytherapy seed placement under mri guidance," *IEEE Transactions on Biomedical Engineering*, vol. 54, pp. 1499–1506, August 2007.

[12] K. Chinzei and K. Miller, "MRI guided surgical robot," in *Australian Conference on Robotics and Automation*, (Sydney, Australia), pp. 50–55, November 2001.

[13] F. Vecchi, C. Freschi, S. Micera, A. Sabatini, and P. Dario, "Experimental evaluation of two commercial force sensors for applications in biomechanics and motor control," in *International Functional Electrical Stimulation Society (IFESS)*, (Aalborg, Danemark), June 2000.

[14] E. Dégoulange, *Commande en effort d'un robot manipulateur à deux bras : application au contrôle de la déformation d'une chaîne cinématique fermée*. PhD thesis, Universit Montpellier II, Montpellier, 1993.